ROYAL SOCIETY OF CHEMISTRY

www.rsc.org/advances
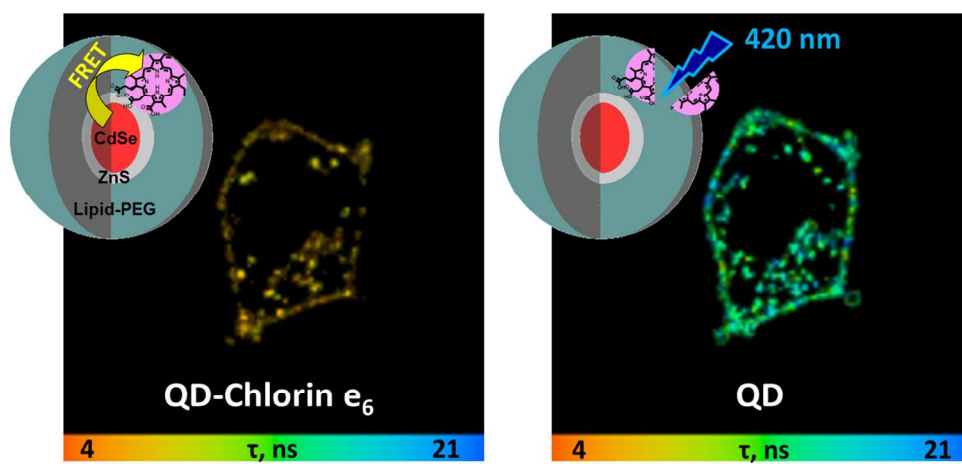
Non-covalent complex of lipid-coated CdSe/ZnS quantum dots and second-generation photosensitizer, chlorin e6 can enter living HeLa cells with maintained integrity that ensures efficient FRET.
228x112mm (150 x 150 DPI)

Journal Name

ARTICLE

Non-covalent complex of quantum dots and chlorin e$_6$: efficient energy transfer and remarkable stability in living cells revealed by FLIM

Jurga Valanciunaite,[a,b] Andrey S. Klymchenko,*[c] Artiom Skripka,[a] Ludovic Richert,[c] Simona Steponkiene,[a,d] Giedre Streckyte,[e] Yves Mely[c] and Ricardas Rotomskis*[a,d]

Forster resonance energy transfer (FRET) system of semiconductor quantum dots and porphyrins represents a new promising photosensitizing tool for photodynamic therapy of cancer. In this work, we demonstrate the ability of non-covalent complex formed between commercial lipid-coated CdSe/ZnS quantum dots (QD) bearing different terminal groups (carboxyl, amine or non-functionalized) and second-generation photosensitizer, chlorin e$_6$ (Ce$_6$) to enter living HeLa cells with maintained integrity and perform FRET from two-photon excited QD to bound Ce$_6$ molecules. Spectroscopic changes, the highly efficient FRET, observed upon Ce$_6$ binding to QD, and remarkable stability of the QD-Ce$_6$ complex in different media suggest that Ce$_6$ penetrates inside lipid coating close to the inorganic core of QD. Two-photon fluorescence lifetime imaging microscopy (FLIM) on living HeLa cells revealed that QD-Ce$_6$ complexes localize within plasma membrane and intracellular compartments and preserve high FRET efficiency (~50%). The latter was confirmed by recovery of QD emission lifetime after photobleaching of Ce$_6$. The intracellular distribution pattern and FRET efficiency of QD-Ce$_6$ complexes did not depend on the charge of QD terminal groups. Given non-covalent nature of the complex, its exceptional stability *in cellulo* can be explained by combination of hydrophobic interactions and coordination of carboxyl groups of Ce$_6$ with ZnS shell of QD. These findings suggest a simple route to preparation of QD-photosensitizer complexes featuring efficient FRET and high stability *in cellulo* without using time-consuming conjugation protocols.

1 Introduction

Unique optical properties of semiconductor quantum dots (QD) as well as their nano-dimensions, stability and ease of surface modification make these nanoparticles attractive for many biological and medical applications.[1-8] In 2003 Samia et al suggested to exploit QD as resonance energy donors for classical photosensitizers (PS) used in photodynamic therapy (PDT) of cancer.[1] PDT is a treatment that uses a photosensitizing drug, usually porphyrin-type molecules, and the light to cure the cancer.[9] Once the light is applied, the excited molecules of PS generate reactive oxygen species (ROS) that subsequently damage cancer cells. QD are particularly well suited as energy donors for PS due to their size-tunable emission spectrum, high emission quantum yield and long lifetime. Additionally, high extinction coefficient (10^5-10^6 M^{-1}cm^{-1}), broad absorption spectrum and minimal photobleaching enable efficient and prolonged excitation of QD. Furthermore, due to their large two-photon absorption cross section QD could be effectively excited by two-photon

irradiation at wavelengths within the 'optical window' of biological tissues,[10] which usually is not the case for porphyrin-type PS.[11] The energy transmitted from either single or two-photon excited QD to PS is further used for generation of ROS.[1, 12-15] Ultimately, combination of QD and PS offers a new attractive photosensitizing tool for both conventional,[1, 5] and two-photon PDT.[16-19] While significant number of studies on different non-covalent QD-PS systems has been reported to date, the majority of them have focused on assemblies in solutions, based either on electrostatic,[1, 13, 20-22] or coordinational,[23, 24] interactions. Despite the efficient FRET these complexes tend to aggregate,[20-22] or may lose their non-covalently bound PS. Furthermore, stability of such QD-PS complexes in cellular context is questionable and needs to be examined. Covalently coupled QD-PS systems,[14, 17, 25] meet the stability requirements in this respect, however the efficient FRET is hard to achieve, because PS molecules are grafted at the interface between water and the QD coating, which is relatively far from the QD core. Moreover, despite the numerous studies on different QD-PS systems in aqueous

solutions, there are only a few reports on stability and FRET properties of QD-PS systems studied in vitro.[26-28]

In this work, we prepared complexes of commercial CdSe/ZnS QD bearing a lipid-based coating with different terminal groups (carboxyl, amine and non-functionalized) with chlorin e_6 (Ce_6), a well-known second-generation photosensitizer having a high quantum yield of singlet oxygen production (Scheme 1).[29] We obtained exceptionally high FRET efficiency of these complexes, suggesting that Ce_6 is firmly imbedded inside QD lipid coating close to the inorganic core. Most importantly, according to the fluorescence lifetime imaging (FLIM) with two-photon excitation, these QD-Ce_6 complexes readily entered living HeLa cells with maintained efficient FRET, which shows their remarkable stability in the intracellular media.
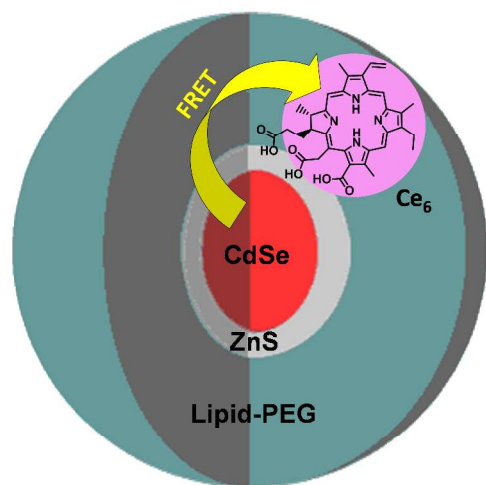
Scheme 1. FRET complex of QD and Ce_6 photosensitizer.

2 Experimental

2.1 Materials

Commercial CdSe/ZnS quantum dots with polyethylene glycol (PEG)-lipid coating (U.S. Pat. No. 7939170) without functional groups (non-functionalized eFluor 625NC), or bearing amine (eFluor 625NC amino) or carboxyl (eFluor 625NC carboxyl) groups, were purchased from eBioscience (USA). The concentration of QD stock solutions provided by manufacturer was 10 µM. Chlorin e_6 tetrasulfonic acid was purchased from Frontier Scientific Inc. (USA). All materials were used without further purification.

2.2 Aqueous solutions

All solutions were prepared in phosphate buffer of pH 7. A stock solution of 1 mM Ce_6 was freshly prepared and further diluted just before the experiments. Working solutions of 0.02 µM QD were prepared by diluting the stock solution of QD 24 hours before the experiments.

QD-Ce_6 solutions were prepared by titrating 2 µl of Ce_6 solution of appropriate concentration into 2 ml of QD solution. In these mixed QD-Ce_6 solutions, the concentration of QD was 0.02 µM, while Ce_6 concentration varied from 0.002 µM to 0.2 µM (QD:Ce_6 molar ratios from 1:0.1 to 1:10 were obtained). To

allow the binding process to reach its equilibrium, the spectra of QD-Ce_6 solutions were measured 20 minutes after QD and Ce_6 were mixed together.

2.3 Characteristics of FRET

Changes in spectral properties of QD and Ce_6 upon QD-Ce_6 complex formation in aqueous solution consisted well with the features of non-radiative dipole-dipole energy transfer mechanism and were evaluated using FRET formalism.[30]
The efficiency of energy transfer (E) was calculated from changes in fluorescence of QD (donor) as follows,

$$E = 1 - \frac{F'_D}{F_D} = 1 - \frac{<\tau'_D>}{<\tau_D>} \tag{1}$$

where F_D and F'_D are the intensities of QD fluorescence in the absence and presence of Ce_6 (acceptor), respectively. $<\tau_D>$ and $<\tau'_D>$ are the amplitude-weighted average lifetimes of QD fluorescence in the absence and presence of Ce_6, respectively.

The quantum yields (QY) of Ce_6 and QD fluorescence were calculated by comparison with Rhodamine B in water (QY_R=31 % at λ_{ex} = 514 nm,[31]) (Table 1 and 2, respectively).

Due to a very low absorbance of Ce_6 at used excitation wavelength (λ_{ex}=465 nm) for FRET measurements, an increase in efficiency of Ce_6 fluorescence in the presence of QD was evaluated using not the QY, but the ratio F'_A/F_A, where F_A and F'_A are the integrated fluorescence intensities of Ce_6 in the absence and presence of QD (donor), respectively. In this case, the change in refractive index of Ce_6 surrounding was not reckoned in.

2.4 Spectroscopic measurements of solutions

Absorption measurements were carried out with Cary 50 spectrophotometer (Varian Inc, USA). The absorption spectra of samples were smoothed using Savitsky-Goaly filter smoothing method.

Fluorescence measurements were performed on Cary Eclipse spectrophotometer (Varian Inc., USA). For the FRET measurements within QD-Ce_6 complex, the excitation at 465 nm was used because only QD could be excited at this wavelength, while the absorption of Ce_6 is minimal (Fig. 1A, dotted arrow). Fluorescence decay was measured with F920 spectrometer (Edinburgh Instruments, UK), equipped with a single photon photomultiplier detector (S900-R). The excitation source was a picosecond pulsed diode laser (EPL-405) with a radiation wavelength at 405 nm and pulse width of 66.9 ps.

Quartz cuvettes with the optical path length of 1 cm were used for absorption and fluorescence measurements.

2.5 HeLa Cells

HeLa cells were grown in Dulbecco's modified Eagle's medium (Gibco-Intvitrogen), supplemented with 10% fetal bovine serum (FBS, Lonza) and 1% penicillin-streptomycin (Gibco-Intvitrogen) at 37°C in a humidified atmosphere containing 5% CO_2. Cells were seeded at a density of 1×10^5 cells per well, 24 hours before incubation. Cells were transferred into a chambered coverglass (Ibidi) with 0.8 mL of the culture medium and then, after 24 h, the medium was substituted with serum-free Opti-MEM (Gibco-Intvitrogen) containing either free QD (0.1 µM), Ce_6 (0.5 µM) or QD-Ce_6 complexes (QD:Ce_6, 1:5, c_{QD}=0.1 µM). The treated cells were kept in the incubator at 37 °C for 2 h. After 2 h of incubation, the cells were washed with Dulbecco's Phosphate-Buffered
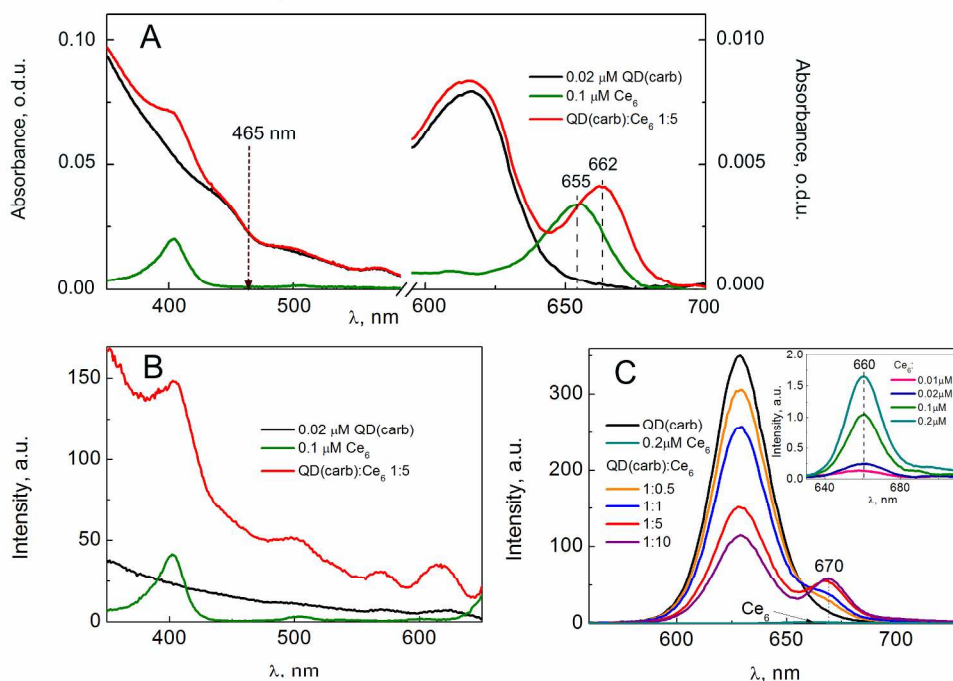
Figure 1. A- absorption and B- fluorescence excitation spectra of 0.02 µM carboxyl QD, 0.1 µM Ce_6 and corresponding mixed QD-Ce_6 (0.02 µM QD : 0.1 µM Ce_6) aqueous solutions. C- fluorescence spectra of 0.02 µM carboxyl QD, 0.2 µM Ce_6 and mixed QD-Ce_6 aqueous solutions at increasing QD:Ce_6 molar ratio from 1:0.5 to 1:10. The dotted arrow in absorption spectra (A) shows the excitation at 465 nm, used for the fluorescence (C) measurements. The inset of Figure C shows the fluorescence of pure Ce_6 solution at corresponding concentrations at λ_{ex} =465 nm. The fluorescence excitation spectra (B) were recorded at the fluorescence maximum of QD-Ce_6 complex at λ_{em}=670 nm.

Saline (DPBS), supplemented with Opti-MEM and immediately imaged by two-photon laser scanning microscope.

2.6 Fluorescence lifetime imaging microscopy in living cells

FLIM experiments on HeLa cells were performed by using a home-built two-photon laser scanning setup based on an Olympus IX70 inverted microscope with an Olympus 60x1.2NA water immersion objective. Two-photon excitation was provided by a titanium-sapphire laser (Tsunami, Spectra Physics) that operated at 830 nm with 5 mW excitation power. Detection system consisted of Avalanche Photodiodes (APD SPCM-AQR-14-FC, Perkin-Elmer) connected to a counter/timer PCI board (PCI6602, National Instrument). The filter of 605 nm with bandwidth of 30 nm was used to exclude the fluorescence of Ce_6. Irradiation of the samples was performed by a blue light (bandpass filter 420/50 nm) for 30 s.

3 Results and discussion

3.1 Steady-state spectral characteristics in aqueous solution

Addition of Ce_6 produced significant changes in absorption and fluorescence spectra of buffered aqueous solutions of carboxyl, amine and non-functionalized QD (Fig. S1 and Fig. S2, respectively). These changes were quite similar for all three different QD. The representative absorption, fluorescence excitation and fluorescence spectra of carboxyl QD solution mixed with different Ce_6 amounts are shown in Fig. 1 A, B and C, respectively. The absorption spectra of QD-Ce_6 solutions did not show simple superposition of corresponding free QD and

Ce_6 spectra (Fig. 1A). The most pronounced difference was seen for Ce_6 Q (I) absorption band, which in the presence of QD shifted from 655 nm to 662 nm. The absorbance of this red-shifted band was higher than that of free Ce_6. Furthermore, in QD-Ce_6 fluorescence spectrum, besides QD emission at 625 nm, the fluorescence band at 670 nm appeared (Fig. 1C) which could be assigned to Ce_6 molecules bound to QD. The successive titration with Ce_6 resulted in the fluorescence intensity decrease of all three types of QD emission at 625 nm and simultaneous increase in fluorescence intensity at 670 nm (Fig. 1C and Fig. S2 B, D, G), which indicates the energy transfer from excited QD to bound Ce_6 molecules. Quite similar absorption and fluorescence characteristics of Ce_6 obtained upon binding to differently charged QD exclude the electrostatic interaction with QD lipid surface as a driving force for the QD-Ce_6 complex formation. Moreover, from the red-shift of Ce_6 Q (I) absorption and fluorescence bands we can state that Ce_6 molecules within QD coating are situated in the hydrophobic microenvironment, most likely, hydrophobic part of QD lipids. This was confirmed by the absorption and fluorescence measurements of Ce_6 in the presence of 5% Triton-X 100, that is a well-known nonionic surfactant forming micelles above 0.02% (critical micelle concentration). Addition of Triton-X 100 to aqueous solution of Ce_6 produced precisely the same red-shift of its absorption and fluorescence bands as in the case of QD (Fig. S3 A and B, respectively and Table 1). The same bathochromic shift of Ce_6 fluorescence maximum to 670 nm was also reported for Ce_6 in the presence of lipid bilayers.[32, 33]

Using excitation at 400 nm, where both bound to QD and free Ce_6 can be efficiently excited, the red-shifted emission at

670 nm was observed for range of Ce$_6$/QD ratios 0.5-5, without signs of unbound Ce$_6$ at 660 nm (Fig. S4). Therefore, in these conditions the binding of Ce$_6$ to QD is probably complete, which is in agreement with our earlier studies.[34] At Ce$_6$/QD ratios ≥10 a contribution of the unbound Ce$_6$ species at 660 nm could be detected probably due to the saturation of the QD binding sites.

Table 1. Spectral characteristics of Ce$_6$ in buffer, 5% Triton-X 100 and bound to QD (in buffer)

Medium	Absorption maximum of Q (I) band, nm	Fluorescence maximum, nm	QY^a, %	F′$_A$/F$_A$ ^{c}
Buffer pH 7	655	660	4.7	1
QD (carb): Ce$_6$ 1:1	662	670	-	113
QD (amine):Ce$_6$ 1:1	662	670	-	91
QD (non-func):Ce$_6$ 1:1	662	670	-	108
5% Triton-X 100	665	670	5.0^b	1.2

^{a}λ$_{ex}$=400 nm, ^{b}n=1.47, ^{c}λ$_{ex}$=465 nm
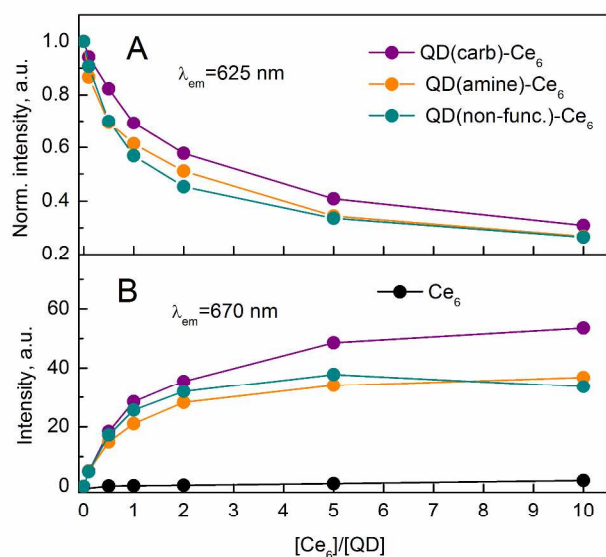
Figure 2. A- Normalized emission intensity of pure QD and mixed QD-Ce$_6$ solutions at increasing QD:Ce$_6$ molar ratios measured at 625 nm. The normalization was performed to the maximum of carboxyl QD emission intensity. B- Absolute intensities of bound Ce$_6$ at 670 nm in QD-Ce$_6$ solutions. For the comparison, the rise in Ce$_6$ intensity at 660 nm due to increasing concentration is also shown.

Remarkably, the fluorescence intensity of Ce$_6$ in complex with QD was ~100-fold larger than that of free Ce$_6$ in buffer directly excited at the same wavelength (465 nm) (Table 1). Changes in the environment of Ce$_6$ from buffer to QD lipid coating cannot explain this increase, as could be seen from minor variation in QY of Ce$_6$ from buffer to 5% Triton-X 100 (Table 1) or lipid membranes.[32] Therefore, the observed drastic fluorescence enhancement clearly points to FRET from QD, which function as an efficient energy antenna. Indeed, at 465 nm excitation wavelength, the extinction coefficient of QD is

>100-fold higher than that of Ce$_6$, and thus the efficient fluorescence of Ce$_6$ originates from the energy transferred from QD.

Moreover, the fluorescence excitation spectra of mixed QD-Ce$_6$ aqueous solutions registered at 670 nm displayed the contribution of both QD and Ce$_6$ spectra, but the intensity of QD-Ce$_6$ solutions was much higher than the sum of the fluorescence intensities of separate components at corresponding concentrations (Fig. 1B and Fig. S2 A, C, E), which confirmed that QD significantly contribute to the fluorescence of bound Ce$_6$ molecules via energy transfer.

The quenching of QD emission intensity by increasing concentration of Ce$_6$ was slightly faster for amine and non-functionalized QD than for carboxyl QD (Fig. 2A). Furthermore, none of QD intensity decrease reached a plateau even at highest used Ce$_6$ concentrations. In contrast, the intensity of bound Ce$_6$ fluorescence band at 670 nm reached its maximum around Ce$_6$/QD =5-10 for three studied QD (Fig. 2B). Further increase in Ce$_6$ concentration resulted in a decrease in this band intensity (data not shown). The latter effect could be explained by the self-quenching of bound Ce$_6$ fluorescence due to its high density on the surface of QD. Thus, we consider that 5 Ce$_6$ molecules per QD is an optimal number to obtain QD-Ce$_6$ complexes with the highest energy transfer efficiency but without the negative self-quenching effect. The FRET efficiency calculated from the decrease in intensity of QD emission at Ce$_6$/QD = 1 and 5 are given in Table 2.

The stability of QD-Ce$_6$ complex over time was studied in aqueous medium of different pH, in phosphate buffer saline (PBS) and in the presence of bovine serum albumin (BSA) (QD:Ce$_6$:BSA 1:5:200) (Fig. 3). In acidic medium (pH 4-6), which should mimic the endosomal/lysosomal compartments of the cells, QD(carb)-Ce$_6$ complex was extremely stable as the FRET efficiency of the QD(carb)-Ce$_6$ complex did no change for 24 hours. In phosphate buffer pH 7.0 and PBS, only a slight decrease in the FRET efficiency was observed (Fig. 3), so that after 24 hours, it retained 85% and 90% of its initial value in PB and PBS, respectively. Addition of BSA resulted in a partial release of Ce$_6$ from the QD(carb)-Ce$_6$ complex, which reduced its initial efficiency of energy transfer by 13 %.
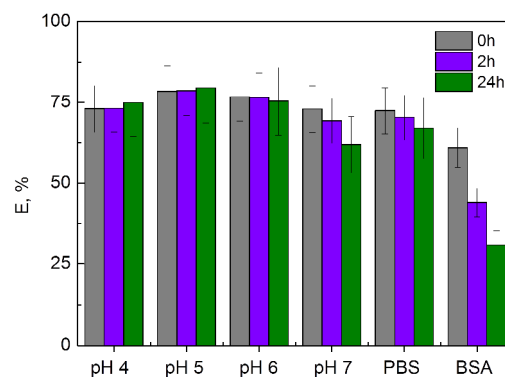
Figure 3. FRET efficiency of QD(carb)-Ce$_6$ complex (1:5) over time in different media. Solutions with varied pH were prepared in 50 mM phosphate buffer. PBS is phosphate buffer saline. BSA is 50 mM phosphate buffer (pH 7.0) containing 4 μM of bovine serum albumin. Concentration of QD was 0.02 μM. The FRET efficiency was calculated from donor intensity at λ$_{em}$=620 nm with λ$_{ex}$=465 nm.

Table 2. FRET properties of QD-Ce$_6$ complexes calculated from the steady-state and time-resolved spectral results in solutions and in HeLa cells.

CdSe/ZnS QD		Steady-state fluorescence measurements in buffer pH 7			Fluorescence decay measurements in buffer pH 7								Two-photon FLIM in HeLa cells
		QD	QD:Ce$_6$ 1:1	QD:Ce$_6$ 1:5	QD	QD:Ce$_6$ 1:1				QD:Ce$_6$ 1:5		QD:Ce$_6$ 1:5
Emission maximum, nm	Terminal groups	QY, %	E, %	E, %	$\langle\tau\rangle$, ns	$\langle\tau\rangle$, ns	E, %	R$_0$, nm	r, nm	$\langle\tau\rangle$, ns	E, %	E*, %
628	carboxyl	26	34	60	16.4	11.1	32	4.2	4.7	6.7	59	45
625	amine	17	39	65	14.2	9.8	30	3.7	4.0	5.9	58	46
628	Non-functionalized	18	43	66	14.6	9.3	36	3.6	3.8	6.1	58	54

*calculated taking $\langle\tau\rangle$ and $\langle\tau'\rangle$ values before cell irradiation, the first and third columns of Fig. 4, respectively.

The release process continued slowly and after 24h, the FRET efficiency of ~30% was still preserved. Thus, addition of BSA produces a burst release of weakly bound Ce$_6$ molecules, while a significant fraction of the photosensitizer remains strongly bound to QD and thus exhibits slow release kinetics.

3.2 Fluorescence decay and FRET in QD-Ce$_6$ complexes

Fig. 4 shows the fluorescence decay profiles of carboxyl QD solution with increasing concentrations of Ce$_6$. They were satisfactorily fitted to a three-exponential decay time model ($0.98 \leq \chi^2 \leq 1.16$) and the obtained average lifetimes of QD decay are summarized in Table 2. The fluorescence decay profile and consequently the average lifetime of QD with different terminal groups varied only slightly: from $\langle\tau\rangle=16.4$ ns for carboxyl QD to $\langle\tau\rangle=14.2$ ns for amine QD (Table 2 and Fig. S5). The increase in concentration of Ce$_6$ substantially shortened the fluorescence decay time of QD (Fig. 4, Fig. S5, Table 2), indicating that efficient FRET occurs. The efficiencies of FRET within QD-Ce$_6$ complexes calculated from the fluorescence decay lifetimes were slightly lower than those obtained from the intensity measurements (Table 2), suggesting that besides FRET some static quenching by bound Ce$_6$ may exist contributing to the emission intensity decrease of QD
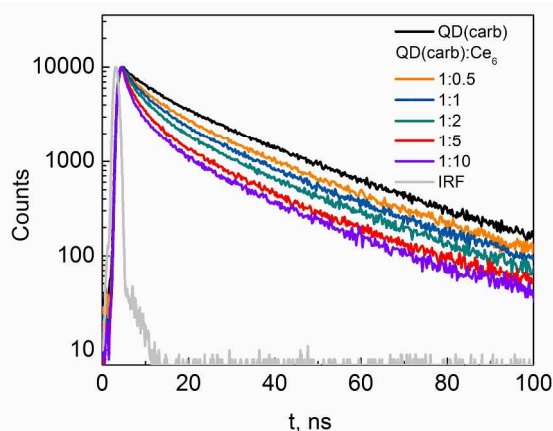
Figure 4. Fluorescence decay of 0.02μm carboxyl QD and carboxyl QD-Ce$_6$ solutions at increasing Ce$_6$ concentration registered at λ_{em}=620 nm with λ_{ex}=405 nm.

without affecting their lifetime. For this reason, we have used

FRET efficiency calculated from time-resolved data to estimate the distance between QD and bound Ce$_6$ molecules (Table 2).

Interestingly, while FRET efficiency values at 1:1 QD:Ce$_6$ ratio for studied QD slightly varied, this difference disappeared at higher Ce$_6$ concentration (QD:Ce$_6$ 1:5) and reached about 60 % for all three types of QD (Table 2). For comparison, in the case of covalent QD-Ce$_6$ conjugate where 26 Ce$_6$ molecules were covalently attached to peptide-coated QD only 50% FRET efficiency was achieved.[14]

The Forster radius (R0) and center-to-center (r) distance between QD and bound Ce$_6$ molecules estimated from the FRET efficiency at 1:1 QD:Ce$_6$ molar ratio are given in Table 2. In these calculations the value of 2/3 for dipole orientation factor (κ2) was used assuming that Ce$_6$ molecules were orientated randomly upon binding to QD. The QD-Ce6 distance ranged from 3.8 nm for non-functionalized QD-Ce$_6$ to 4.7 nm for carboxyl QD-Ce$_6$ pair (Table 2). According to literature, the diameter of QD (eFluor 625 NC) without organic coating is ~ 7.1 nm,[35] while the thickness of PEG-lipid layer from QD hydrodynamic diameter measurements could range from 5 to 9 nm.[35, 36] The center-to-center distance of 3.8-4.7 nm, estimated from FRET data, is close to the shortest possible QD-Ce$_6$ distance that includes ~3.6 nm of QD radius and ~0.5 nm of Ce$_6$ radius. Thus, we can validate that the amphiphilic Ce$_6$ molecules were able to penetrate inside PEG-lipid coating and localize in close proximity to the inorganic core of QD for efficient FRET to occur.

We have also examined time-resolved decay of Ce$_6$ molecules bound to QD (Fig. S6). In the absence of donors, the decay of directly excited Ce$_6$ was single-exponential with the lifetime of 4.3 ns and 5.1 ns in buffer and 5% Triton-X 100, respectively. The decay of bound Ce$_6$ excited via energy transfer from QD became significantly longer and could not anymore be fitted by a monoexponential function (Fig. S6). Within a FRET couple, the apparent decay time of the acceptor Ce$_6$ should contain the decay time of the donor QD, thus explaining the observed phenomenon. Similar elongation of acceptor lifetime was described by Maliwal et al. where long-lifetime lanthanide-based luminophore (donor) resulted in a long-lived component in the covalently linked acceptor decay, which alone displayed a short lifetime.[37]

3.3 Microscopy studies of QD-Ce$_6$ complexes in living HeLa cells

Two-photon FLIM images of HeLa cells treated either with QD alone or QD-Ce$_6$ complexes are shown in Fig. 5. After 2h of incubation with QD alone, strong fluorescence signal was
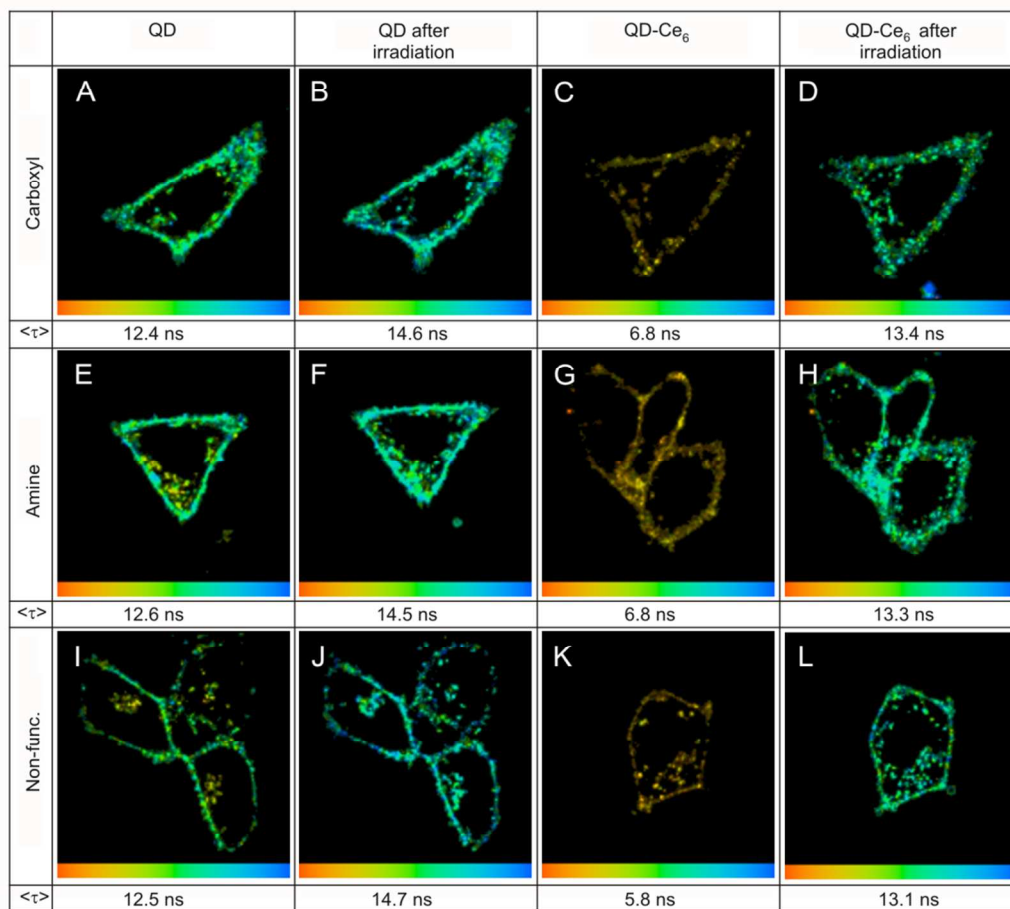
Figure 5. Two-photon FLIM images of HeLa cells incubated for 2 hours with carboxyl (A, B), amine (E, F) and non-funcionalized (I, J) QD and their complexes with Ce_6 (C, G, K and D, H, L) before and after irradiation with blue light for 30 s, respectively. The size of all images is 70x70 μm. The color lifetime scale of each image is from 4 (red) to 21 (blue) nm. <τ> indicates the lifetime of QD emission averaged through the entire image.

observed at the plasma membranes and inside the cells for all three types of QD, whereas the control cells without QD showed no sign of fluorescence at the same experimental conditions (data not shown). Therefore, we can conclude that these QD readily bind and enter living HeLa cells. Despite the difference in surface charge, the pattern of QD distribution inside cells was quite similar: the highest amount of QD concentrated within the plasma membrane while significant fraction of QD was located in the intracellular compartments (Fig. 5 A, E, I). No signal was obtained from the nucleus of the cells. Similarly, other studies have demonstrated that although the charge of terminal groups may determine the pathway and quantity of QD internalization, it does not affect the final intracellular distribution and localization of QD.[38-40] Lately, we have shown that carboxyl QD enter cells via lipid raft/caveolin-mediated endocytosis, accumulate in endosomes and end-up in the multivesicular bodies. [41, 42]

As seen from Fig 5. A, E, I, the emission lifetime of QD in cells was a little shorter than in solutions (Table 2). Moreover, the distribution of QD emission lifetime in cells was not homogeneous. In the plasma membrane the average emission lifetime was rather long (~12.5 ns) while in the intracellular vesicles it was by 2-6 ns shorter (Fig. 5 A, E, I). Irradiation of the cells by a blue light for 30 s enhanced the emission intensity of QD and lengthened its lifetime by ~2 ns in average.

Remarkably, the obtained lifetime values were close to those for QD in solutions (Fig. 5 B, F, J and Table 2), thus confirming that the observed cellular fluorescence belongs to QD. Moreover, after irradiation, the difference between emission lifetime of QD in plasma membranes and those in the intracellular compartments reduced. Shortening of fluorescence lifetime of thiol-capped CdTe QD inside living cells was reported by Zhang et al, who demonstrated in solutions that both, reduction of pH and interaction with different amino acids and proteins may be responsible.[43, 44] In our case, almost complete recovery of QD fluorescence lifetime after irradiation suggests that QD might be quenched by a blue light absorbing intracellular chromophores, such as NADH, flavins, quinones, and other cofactors or even endogenous porphyrins. The direct excitation by a blue light causes their photobleaching and thus recovers almost completely the QD properties.

FLIM images of QD-Ce_6 complexes (QD:Ce_6 1:5) incubated for 2h with HeLa cells before and after irradiation are shown in the third and fourth columns of Fig. 5, respectively. Similarly to QD alone, most of QD-Ce_6 complexes accumulated in the plasma membrane and fewer in the intracellular compartments. The fluorescence lifetime of QD-Ce_6 complexes was the half (5.8-6.8 ns) of the QD, which matches perfectly with the time-resolved data of these complexes in solutions (Table 2). Hence, QD-Ce_6 complexes in

cells preserved the high FRET efficiency (Table 2). Photobleaching of Ce_6 (FRET acceptor) by irradiation of the cells with the blue light for 30 s resulted in the recovery of the large values of the emission lifetime (Fig. 5 D, H, L) close to that of the irradiated QD without Ce_6. These results show that QD complexes with Ce_6 after internalization into HeLa cells remain stable in the cellular context and do not change their composition. This is a striking result, taking into account that Ce_6 molecules are known to readily bind different proteins and cellular membranes, including the plasmatic, nuclear and mitochondrial membranes.[33, 45] The absence of leakage of Ce_6 molecules from QD into cellular membrane components indicates exceptionally strong binding between QD and Ce_6. Hydrophobic interactions with lipid coating could be one possible explanation for this phenomenon, as amphiphilic Ce_6 seems to localize in the apolar lipid environment of QD. From the simple geometric consideration, taking into account the QD diameter of 20 nm and a typical surface area per lipid of 0.7 nm^2, the estimated number of lipids per QD is <1800, so that the lipid concentration for the 0.02 µM solution of QD was <36 µM. Taking into account the relatively low affinity constant of Ce_6 to vesicles of unsaturated lipids (dioleoylphosphatidylcholine) at pH 7.4 (6×10^3 M^{-1}),[33] only <18 % of Ce_6 should be bound to lipids of QD at the Ce_6/QD ratios used. However, the observation of highly efficient FRET at 1:1 complex and our titration data suggest nearly quantitative binding of Ce_6 to QD. Moreover, taking into account that the affinity of Ce_6 to BSA (1.8×10^8 M^{-1}),[33] is about ~30000-fold higher than that to lipid membranes, the QD-Ce_6 complex should be readily destroyed in the presence of BSA excess. However, the opposite was observed, so that the release of Ce_6 from QDs to BSA was very slow and incomplete (Fig. 3), in line with the earlier work.[46] Therefore, the hydrophobic interactions of Ce_6 with lipids of QD cannot be the only reason for this exceptional stability of the complexes in biological media. We speculate that due to its three carboxyl groups Ce_6 could interact directly with ZnS layer of the QD core (Scheme 1). For instance, Patel et al. showed that in oleic acid-capped ZnS semiconducting nanocrystals, the two oxygen atoms of the carboxylate were coordinated symmetrically to the surface of the nanorystals, thus providing high stability to the formed fatty acid monolayers and to the obtained nanocrystals colloids.[47] Such bonding of Ce_6 carboxyl groups to ZnS layer of QD could also explain the unexpectedly high values of FRET efficiency, indicating that deeply imbedded in the QD lipid coating Ce_6 molecules situate very close to QD inorganic core.

Conclusions

The use of QD as FRET donors can drastically improve the excitation efficiency of the photosensitizer. Here, we studied formation of complexes between QD bearing neutral, carboxyl and amine functional groups with second-generation photosensitizer, chlorin e6. Spectroscopic changes and the highly efficient FRET, observed upon Ce_6 binding to QD, suggest that Ce_6 localizes inside lipid coating close to the inorganic core of QD. Two-photon fluorescence lifetime imaging microscopy on living HeLa cells revealed that, independently of QD surface functional groups, QD-Ce_6 complexes localize within plasma membrane and intracellular compartments and preserve ~50% FRET efficiency. This exceptional stability *in cellulo* of non-covalent QD-Ce_6 complexes can be explained by coordination of carboxyl groups of Ce_6 with ZnS shell of QD, in addition to hydrophobic interactions. Our data suggest that a simple protocol without chemical conjugation can lead of QD-photosensitizer complexes characterized by efficient FRET and excellent stability *in cellulo*.

Notes and references

[a] Biomedical Physics Laboratory, Institute of Oncology, Vilnius University, P. Baublio 3b, LT-08406, Vilnius, Lithuania.
[b] Baltic Institute of Advanced Technology, Sauletekio 15, LT-10224, Vilnius, Lithuania.
[c] University of Strasbourg, CNRS, UMR 7213, Laboratory of Biophotonics & Pharmacology, Faculty of Pharmacy, F-67401 Illkirch Graffenstaden, France.
[d] Laser Research Center, Vilnius University, Sauletekio 9, bldg. 3, LT-10222 Vilnius, Lithuania

*Corresponding authors: ASK, Tel: +33 368 85 42 55, Fax: +33 368 85 43 13, E-mail: andrey.klymchenko@unistra.fr; RR, Tel: +370 5 2190908, ricardas.rotomskis@vuoi.lt

Electronic Supplementary Information (ESI) available: additional steady-state and time-resolved spectroscopy data. See DOI: 10.1039/b000000x/

1   A. C. S. Samia, X. B. Chen and C. Burda, *Journal of the American Chemical Society*, 2003, **125**, 15736-15737.

2   X. Michalet, F. F. Pinaud, L. A. Bentolila, J. M. Tsay, S. Doose, J. J. Li, G. Sundaresan, A. M. Wu, S. S. Gambhir and S. Weiss, *Science*, 2005, **307**, 538-544.

3   I. L. Medintz, H. T. Uyeda, E. R. Goldman and H. Mattoussi, *Nature Materials*, 2005, **4**, 435-446.

4   A. P. Alivisatos, W. W. Gu and C. Larabell, *Annual Review of Biomedical Engineering*, 2005, **7**, 55-76.

5   P. Juzenas, W. Chen, Y. P. Sun, M. A. N. Coelho, R. Generalov, N. Generalova and I. L. Christensen, *Advanced Drug Delivery Reviews*, 2008, **60**, 1600-1614.

6   I. L. Medintz and H. Mattoussi, *Physical Chemistry Chemical Physics*, 2009, **11**, 17-45.

7   B. A. Kairdolf, A. M. Smith, T. H. Stokes, M. D. Wang, A. N. Young and S. Nie, *Annual review of analytical chemistry (Palo Alto, Calif.)*, 2013, **6**, 143-162.

8   C. E. Probst, P. Zrazhevskiy, V. Bagalkot and X. Gao, *Advanced drug delivery reviews*, 2013, **65**, 703-718.

9   T. J. Dougherty, C. J. Gomer, B. W. Henderson, G. Jori, D. Kessel, M. Korbelik, J. Moan and Q. Peng, *Journal of the National Cancer Institute*, 1998, **90**, 889-905.

10 D. R. Larson, W. R. Zipfel, R. M. Williams, S. W. Clark, M. P. Bruchez, F. W. Wise and W. W. Webb, *Science*, 2003, **300**, 1434-1436.

11 A. Karotki, M. Drobizhev, M. Kruk, C. Spangler, E. Nickel, N. Mamardashvili and A. Rebane, *Journal of the Optical Society of America B-Optical Physics*, 2003, **20**, 321-332.

12 E. I. Zenkevich, E. I. Sagun, V. N. Knyukshto, A. S. Stasheuski, V. A. Galievsky, A. P. Stupak, T. Blaudeck and C. von Borczyskowski, *Journal of Physical Chemistry C*, 2011, **115**, 21535-21545.

RSC Advances Accepted Manuscript

13 L. X. Shi, B. Hernandez and M. Selke, *Journal of the American Chemical Society*, 2006, **128**, 6278-6279.

14 J. M. Tsay, M. Trzoss, L. X. Shi, X. X. Kong, M. Selke, M. E. Jung and S. Weiss, *Journal of the American Chemical Society*, 2007, **129**, 6865-6871.

15 C. Fowley, N. Nomikou, A. P. McHale, P. A. McCarron, B. McCaughan and J. F. Callan, *Journal of Materials Chemistry*, 2012, **22**, 6456-6462.

16 Y. N. Wen, W. S. Song, L. M. An, Y. Q. Liu, Y. H. Wang and Y. Q. Yang, *Applied Physics Letters*, 2009, **95**.

17 Z. D. Qi, D. W. Li, P. Jiang, F. L. Jiang, Y. S. Li, Y. Liu, W. K. Wong and K. W. Cheah, *Journal of Materials Chemistry*, 2011, **21**, 2455-2458.

18 L. M. An, K. F. Chao, Q. H. Zeng, X. T. Han, Z. Yuan, F. Xie, X. Fu and W. Y. An, *Journal of Nanoscience and Nanotechnology*, 2013, **13**, 1368-1371.

19 A. Skripka, J. Valanciunaite, G. Dauderis, V. Poderys, R. Kubiliute and R. Rotomskis, *Journal of Biomedical Optics*, 2013, **18**.

20 A. O. Orlova, V. G. Maslov, A. A. Stepanov, I. Gounko and A. V. Baranov, *Optics and Spectroscopy*, 2008, **105**, 889-895.

21 M. Idowu and T. Nyokong, *Spectrochimica Acta Part a-Molecular and Biomolecular Spectroscopy*, 2010, **75**, 411-416.

22 P. M. Keane, S. A. Gallagher, L. M. Magno, M. J. Leising, I. P. Clark, G. M. Greetham, M. Towrie, Y. K. Gun'ko, J. M. Kelly and S. J. Quinn, *Dalton Transactions*, 2012, **41**, 13159-13166.

23 E. Zenkevich, F. Cichos, A. Shulga, E. P. Petrov, T. Blaudeck and C. von Borczyskowski, *Journal of Physical Chemistry B*, 2005, **109**, 8679-8692.

24 S. Dayal, R. Krolicki, Y. Lou, X. Qiu, J. C. Berlin, M. E. Kenney and C. Burda, *Applied Physics B-Lasers and Optics*, 2006, **84**, 309-315.

25 G. Charron, T. Stuchinskaya, D. R. Edwards, D. A. Russell and T. Nann, *Journal of Physical Chemistry C*, 2012, **116**, 9334-9342.

26 A. Rakovich, D. Savateeva, T. Rakovich, J. F. Donegan, Y. P. Rakovich, V. Kelly, V. Lesnyak and A. Eychmuller, *Nanoscale Research Letters*, 2010, **5**, 753-760.

27 L. Li, J. F. Zhao, N. Won, H. Jin, S. Kim and J. Y. Chen, *Nanoscale Research Letters*, 2012, **7**.

28 E. Yaghini, F. Giuntini, I. M. Eggleston, K. Suhling, A. M. Seifalian and A. J. MacRobert, *Small*, 2014, **10**, 782-792.

29 J. M. Fernandez, M. D. Bilgin and L. I. Grossweiner, *Journal of Photochemistry and Photobiology B-Biology*, 1997, **37**, 131-140.

30 J. R. Lakowitcz, *Principles of Fluorescence Spectroscopy*, Springer Science+Business Media, New York, 1999.

31 D. Magde, G. E. Rojas and P. G. Seybold, *Photochemistry and Photobiology*, 1999, **70**, 737-744.

32 A. A. Frolov, E. I. Zenkevich, G. P. Gurinovich and G. A. Kochubeyev, *Journal of Photochemistry and Photobiology B: Biology*, 1990, **7**, 43-56.

33 H. Mojzisova, S. Bonneau, C. Vever-Bizet and D. Brault, *Biochimica Et Biophysica Acta-Biomembranes*, 2007, **1768**, 366-374.

34 J. Valanciunaite, A. Skripka, G. Streckyte and R. Rotomskis, Complex of water-soluble CdSe/ZnS quantum dots and chlorin e6: interaction and FRET, Oulu, 2010.

35 T. L. Jennings, S. G. Becker-Catania, R. C. Triulzi, G. L. Tao, B. Scott, K. E. Sapsford, S. Spindel, E. Oh, V. Jain, J. B. Delehanty, D.

E. Prasuhn, K. Boeneman, W. R. Algar and I. L. Medintz, *Acs Nano*, 2011, **5**, 5579-5593.

36 A. M. Dennis, D. C. Sotto, B. C. Mei, I. L. Medintz, H. Mattoussi and G. Bao, *Bioconjugate Chemistry*, 2010, **21**, 1160-1170.

37 B. P. Maliwal, Z. Gryczynski and J. R. Lakowicz, *Analytical Chemistry*, 2001, **73**, 4277-4285.

38 T. A. Kelf, V. K. A. Sreenivasan, J. Sun, E. J. Kim, E. M. Goldys and A. V. Zvyagin, *Nanotechnology*, 2010, **21**.

39 J. Park, J. Nam, N. Won, H. Jin, S. Jung, S. Jung, S. H. Cho and S. Kim, *Advanced Functional Materials*, 2011, **21**, 1558-1566.

40 M. J. D. Clift, C. Brandenberger, B. Rothen-Rutishauser, D. M. Brown and V. Stone, *Toxicology*, 2011, **286**, 58-68.

41 L. Damalakiene, V. Karabanovas, S. Bagdonas, M. Valius and R. Rotomskis, *International Journal of Nanomedicine*, 2013, **8**, 555-568.

42 V. Karabanovas, Z. Zitkus, D. Kuciauskas, R. Rotomskis and M. Valius, *Journal of Biomedical Nanotechnology*, 2014, **10**, 775-786.

43 Y. Zhang, L. Mi, P. N. Wang, S. J. Lu, J. Y. Chen, J. Guo, W. L. Yang and C. C. Wang, *Small*, 2008, **4**, 777-780.

44 Y. Zhang, L. Mi, J. Y. Chen and P. N. Wang, *Biomedical Materials*, 2009, **4**.

45 R. Bachor, C. R. Shea, R. Gillies and T. Hasan, *Proceedings of the National Academy of Sciences of the United States of America*, 1991, **88**, 1580-1584.

46 A. Skripka, J. Valanciunaite and R. Rotomskis, *Medical Physics in the Baltic States*, 2010, 59-61.

47 J. D. Patel, F. Mighri and A. Ajji, *Materials Research Bulletin*, 2012, **47**, 2016-2021.